

The dynamics of two air bubbles loaded by an underwater shock wave

著者	小玉 哲也
journal or publication title	Journal of Applied Physics
volume	80
number	10
page range	5587-5592
year	1996
URL	http://hdl.handle.net/10097/47481

doi: 10.1063/1.363605

The dynamics of two air bubbles loaded by an underwater shock wave

T. Kodama^{a)} and K. Takayama

Shock Wave Research Center, Institute of Fluid Science, Tohoku University, 2-1-1 Katahira, Aoba Ward, Sendai 980-77, Japan

N. Nagayasu

Chugoku Kayaku CO., LTD 5-1-1 Etajima-cho, Aki-gun, Hiroshima 737-21, Japan

(Received 22 April 1996; accepted for publication 19 August 1996)

An experimental study has been made on the interaction of an underwater shock wave with two air bubbles attached to a gelatin surface. The shock wave was generated by detonating a microexplosive pellet, and the subsequent behavior of bubble collapse was visualized by high-speed photography. By measuring the directivity and the maximum depth of the liquid jets of the two bubbles penetrating into the gelatin, it was found that when the bubbles are beyond a critical separation distance, the depth of the penetration was no longer affected by the presence of the other bubble, and that the penetration depth for a given bubble in a two-bubble arrangement is a function of the size of the other bubble. © 1996 American Institute of Physics. [S0021-8979(96)06522-X]

I. INTRODUCTION

Cavitation erosion in hydraulic machinery,¹⁻⁸ ignition of slurry explosions,^{9,10} and side effects associated with extracorporeal shock wave lithotripsy treatment^{11,12} are mainly caused by impulsive pressures resulting from cavitation bubble collapses. Shock waves and liquid jets are produced for a very short time during the bubble collapse, and the resultant impulsive pressures cause damage to the surrounding materials. In practical cases, where cavitation or two-phase flow occurs, cavitation bubbles seldom exist as a single bubble, and as a result they interact with each other. This is especially so in cases where clouds of bubbles exist.

Theoretical and experimental studies confirmed that the impulsive pressure generated by a multiple interaction can be much higher than that caused by a single bubble. Hansson and Mørch¹ showed that the collapse of a cavity cluster driven by the ambient pressure continues from the outer boundary of the cluster towards its center, causing pressure rises significantly above the ambient level. Sanada *et al.*² observed multiple shock waves in the ultrasound field by means of holographic interferometry. Tomita *et al.*³ investigated the effects of the number and configuration of gas bubbles in the process of the bubble collapse and the generation of the impulsive pressure. Dear and Field⁶ studied the collapse of arrays of cavities using high-speed photography. Recently, Testud-Giovanneschi *et al.*⁷ visualized bubble-bubble and bubble-shock wave interaction. Kodama *et al.*⁸ investigated the interaction of two collapsing bubbles with a free surface. The main purpose of these studies was to find the optimum condition in which bubbles collapse most violently due to their mutual interactions.

In the present article the interaction of two collapsing bubbles was considered. The bubbles were attached to a gelatin surface, and then loaded by an underwater shock wave. The gelatin has about the same acoustic impedance as that of water, thus the bubbles can be regarded as being placed in a uniform medium. From observations regarding

the direction and penetration depth of liquid jets formed within the two bubbles penetrating into the gelatin, the critical interaction distance and the optimal condition in which a larger bubble collapses most violently due to its interaction with a smaller bubble was deduced.

II. EXPERIMENTAL EQUIPMENT AND PROCEDURE

A schematic description of the experimental setup is shown in Fig. 1. Experiments were conducted in a stainless-steel chamber (245×345×400 mm³). The chamber was filled with tap water at room temperature, $T_{\infty}=291$ K, under atmospheric pressure, $P_{\infty}=101.5$ kPa. The water surface tension was measured to be 7.2×10^{-2} N m⁻¹.¹³ The water was supplied into the chamber through a filter of 5 μ m elements.

A gelatin block was used to observe the characteristics of the formation of liquid jets produced within bubbles. The gelatin was dissolved 10% by weight of gelatin in water at 333 K and then cast in a mold. The mold surfaces were covered with a thin plastic film. After a slow cooling to reduce shrinkage, the gelatin layer was cut out in pieces. The acoustic impedance of the gelatin surface is 1.62×10^6 kg m⁻² s⁻¹ (at 294 K).¹⁴ The gelatin surface was immersed in water and the immersion time of the gelatin in the water was restricted to be less than 10 min in order to keep the degree of swelling of the gelatin constant. According to acoustic theory, about 99.8% of the transmitted sound wave pressure amplitude is transferred to the gelatin. Therefore, the effect of wave reflection from the gelatin surface on the bubble collapse may be neglected and it is assumed that the two bubbles exist in an almost uniform medium. There is no difference in the behavior of the bubble when the thickness of the gelatin is over 6 mm, thus the bubble collapse is assumed to be independent of the gelatin thickness, unless its width is extremely small. Therefore, 10-mm-thick gelatin plates were used.

Two air bubbles with a given size were carefully placed under the gelatin surface using a syringe. The distance between these bubbles was 2S. A 10.0 ± 0.1 mg silver azide pellet (Chugoku Kayaku Co., Ltd.) was used to produce the

^{a)}Electronic mail: kodama@ifs.tohoku.ac.jp

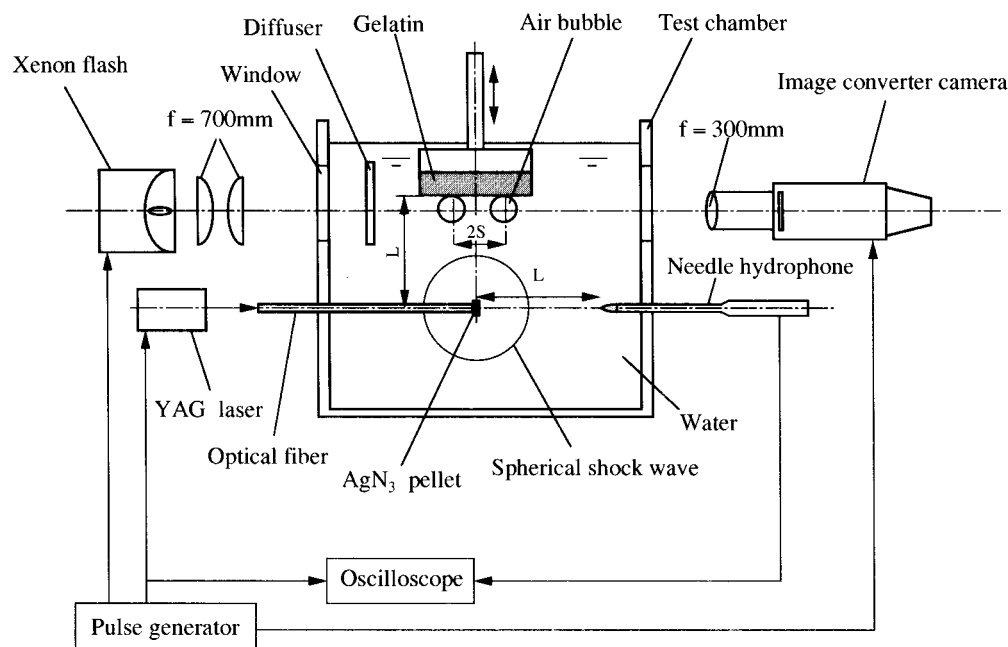


FIG. 1. Experimental arrangement for high-speed photometry.

required shock wave. This pellet was glued to the tip of an optical fiber, 0.4 mm core diameter, and positioned at a stand-off distance of $L=50$ mm from the gelatin surface, on the center axis between the two bubbles. Once the pellet was detonated by a YAG laser beam (Laser photonics, pulse duration 7 ns and 25 mJ/pulse) transmitting through the fiber, a spherical shock wave was produced. This shock wave loaded the two bubbles attached to the gelatin surface. The technique of laser ignition of explosive pellets has been developed at the Shock Wave Research Center of the Institute of Fluid Science, Tohoku University. Takayama *et al.*¹⁵ described in details the production and propagation of spherical shock waves generated by explosive pellets using double exposure holographic interferometry and the random choice method.

A PVDF needle hydrophone (Imotech Meßtechnik 300/25/48, with a 0.5-mm-diam sensitive element) was placed at a distance L (see Fig. 1) for monitoring the overpressure P_s . The hydrophone was connected to the input of a digitizing oscilloscope [Hewlett Packard 54510A; 1 M Ω (7 pF)]. The measured overpressure at L was $P_s=10.2\pm0.5$ MPa ($n=4$). The shock wave profile at $L=50$ mm from the source is shown in Fig. 2. The rise time was 62.7 ± 1.9 ns ($n=4$). The rise time was defined as the time required for the pressure to increase from 10% to 90% of its maximum pressure. Using equations derived by Ballhaus and Holt,¹⁶ we can estimate the shock Mach number and the resulting particle speed behind the shock wave at 1.008 and 5.75 m/s, respectively.

The behavior of the collapsing bubbles was photographed using a high-speed camera (Hadland Photonics, Imacon 790) in framing modes; the framing rate was either 25 000 or 1 000 000 frames s^{-1} . A xenon flash lamp with 400 μs pulse duration, was used as a light source. Photo-

graphing was controlled by a three-channel delay generator (Hadland Photonics).

III. RESULTS AND DISCUSSION

A. Interaction of two bubbles having the same diameters

First, the interaction of two bubbles of identical diameters with an underwater shock wave was investigated by varying the distance ($2S$) between the two bubbles. All physical quantities related to the left bubble were denoted by subscript 1 and for the right bubble by 2. In the following study the actual bubble, produced using a syringe, had a nonperfect spherical symmetry. It was, therefore, treated as an equivalent sphere having the same volume as the original bubble.

In Fig. 3 the collapse of two bubbles of equal diameter (D) is recorded. In each set of photographs a separate frame,

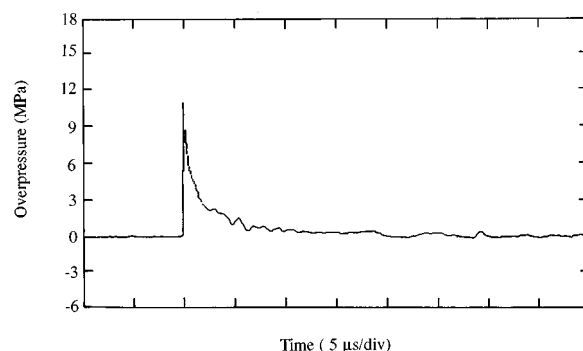


FIG. 2. Shock wave profile at $L=50$ mm from the shock wave source.

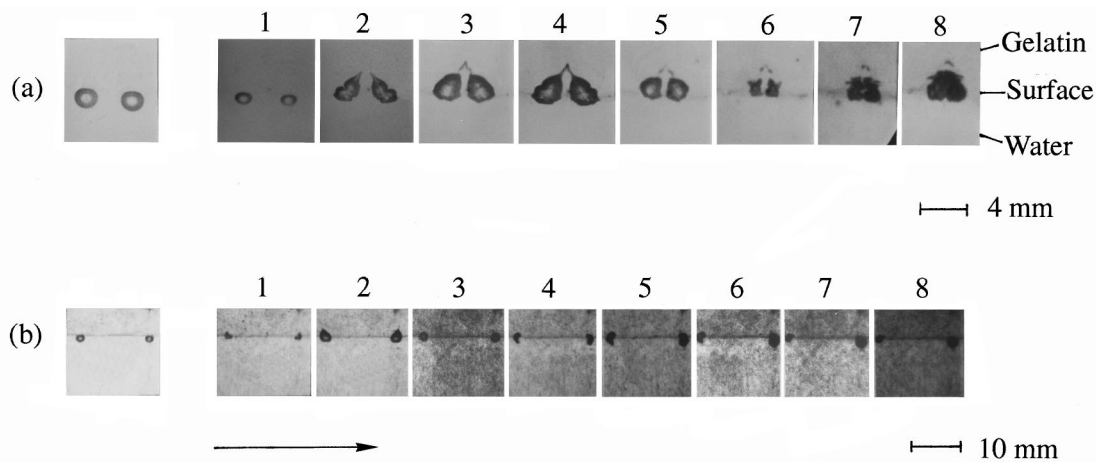


FIG. 3. Two bubbles collapsing by an underwater shock wave loading: $P_s = 10.2 \pm 0.5$ MPa. Interframe time $40 \mu\text{s}$ and exposure is $8.0 \mu\text{s}/\text{frame}$. (a) $D_1 = 1.85$ mm, $D_2 = 1.85$ mm, $2S = 4.09$ mm. (b) $D_1 = 1.88$ mm, $D_2 = 1.88$ mm, $2S = 16.1$ mm.

shown on the left side, indicates the initial stationary state of the bubbles. The propagation direction of the shock wave was vertically upward, along the symmetry line between the bubbles. Impinged by the shock wave, the two bubbles were in the rebound phase during the first frame shown in Fig. 3.

Figure 3(a) shows the collapse of the two bubbles having a 1.85 mm initial diameter, where $2S$ was 3.70 mm and the interframe time, $40 \mu\text{s}$. The explosive generated shock wave propagates radially, and the pressure behind it decreases inversely with respect to its radius in the same way that pressure decreases below the atmospheric value in a free air blast wave (Fig. 2). After interacting with the two bubbles 15 μs before the first frame of Fig. 3(a), the shock wave is transmitted to the gelatin surface. Meanwhile the two bubbles elongate into the gelatin and toward each other with a cone-shaped elongation, then shrink and join. The liquid jet formed within each bubble is shown in the second frame of Fig. 3(a). These jets continue to penetrate into the gelatin against the resisting force between the jets and the gelatin, and finally come to a stop, intersecting each other at the central axis [third frame in Fig. 3(a)]. Subsequently the two bubbles grow, pushing against the gelatin in a triangular shape, then merge with each other at the seventh frame of Fig. 3(a). The gelatin was recovered after the experiment and measurements made. There were two holes detected at the position on the gelatin where the bubbles were placed. Therefore, when a liquid jet imparts an impulsive pressure loading which is above the dynamic yield threshold, and it is enough to generate a large plastic deformation, then the kinetic energy of the liquid jet is consumed only by penetrating into the surface. This results in producing a hole in the gelatin plate whose diameter is comparable to the jet diameter.

Figure 3(b) shows bubble collapse when the relative distance is increased, now D_1 and D_2 are equal to 1.88 mm each, $2S$ is equal to 16.1 mm. The direction of each liquid jet is away from the central axis, which is completely different from the result shown in Fig. 3(a). It is plausible to explain this observation by considering the resulting flow field using the image theory¹⁷ and the Bjerknes effect.¹⁸ In the present work, we investigated the direction of liquid jets as a func-

tion of the distance between the bubbles. This was accomplished by changing the distance ($2S$) between the bubbles and while doing so we clarified quantitatively the intensity of the interaction between the bubbles. Let us introduce two functions, θ and ϕ defined in Fig. 4. θ is the angle between the central axis of the left bubble and the direction of the liquid jet formed within this bubble. Angle $\phi = [\tan^{-1}(S/L)]$ describes the direction of movement of the incident shock wave from its central axis. In a case where the two bubbles are placed close to each other, they tend to coalesce. Therefore, there is a critical angle ϕ_c over which the two bubbles can exist separately before the charge is set off. In the present experiment this critical value was $\phi_c = 1.2^\circ$ (shown in Fig. 5 and Fig. 6). This value is probably determined by the bubble diameter and surface tension of the liquid.

Figure 5 illustrates the relation between θ and ϕ , where the solid curve depicts the result of the interaction of two bubbles, while the dashed curve represents that of a single bubble, i.e., the right bubble does not exist, where D_1 and D_2 are equal to 1.88 ± 0.12 mm. In the case of a single bubble, the liquid jet develops in the direction of the incident shock wave, which results in a linear dependence between θ and ϕ .

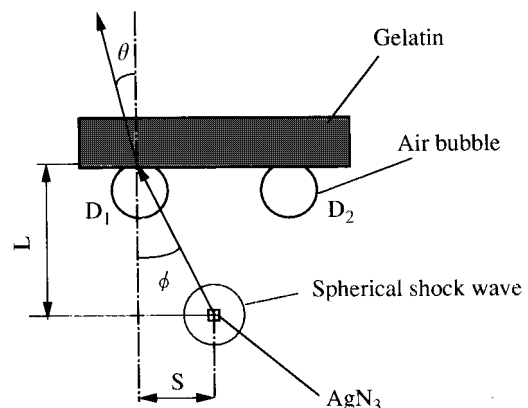


FIG. 4. Geometric parameters describing the incident angle ϕ of the spherical shock wave and the jet angle θ of the collapsing bubble.

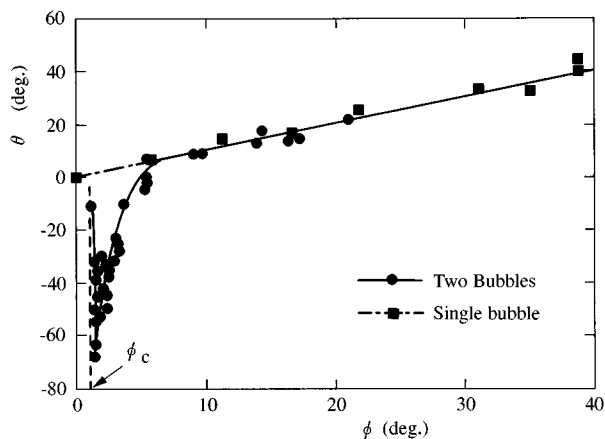


FIG. 5. Relation between the incident angle ϕ and the jet angle θ . $D_1, D_2=1.88\pm0.12$ mm, $P_s=10.2\pm0.5$ MPa. The interaction of two bubbles result is depicted with the solid curve, while the dashed curve represents the single bubble result. The interaction of the two bubbles vanished at a 6° .

In the two bubbles case the angle θ at first rapidly decreases with increasing ϕ up to a minimum value reached at $\phi=1.5^\circ$ which is $\theta=-68^\circ$. At this point, the mutual interaction reaches a maximum. After this minimum the angle θ increases with increasing ϕ , and finally, it coincides with the results obtained for the case of a single bubble (at $\phi=6^\circ$), i.e., there is no two bubble interaction at this angle. This angle corresponds to a separation distance six times larger than the diameter of the initial bubble in the experiment. When $2S$ varies from 1.75 to 5.24 mm, ϕ changes from 1° to 3° . The change of $2S$ is large enough to measure precisely the small changes of ϕ and the rapid change of θ .

Tomita *et al.*³ investigated the interaction between two bubbles attached to a pressure transducer with an underwater shock wave and concluded that there is no two bubbles interaction if the separation distance is four times larger than the initial bubble radius. In the present results the separation distances are three times larger than those reported by Tomita *et al.*³ The deviation can be explained by the fact that Tomita *et al.* employed a pressure transducer with a rise time of $1\ \mu\text{s}$ and an effective diameter of 5.55 mm, therefore the transducer fails to detect the minute concentrated shock loading and the direction of the liquid jet formed within a bubble. Recently, Testud-Giovanneschi *et al.*⁷ reported that the region affected by a bubble is approximately equal to eight times its maximum radius (i.e., the maximum radius of the first oscillation). This conclusion is based on observations of laser-induced-cavitation bubbles in water. However, the laser-induced bubbles interact with the shock waves produced at their initiation and with the source flows generated at their inception, thus it is difficult to compare directly their results with the present findings.

Next, the relationship between the l_1/D_1 and ϕ was considered, where l_1 is the vertical component of the penetration depth attained by the liquid jet of the left bubble whose diameter is D_1 . The obtained results are shown in Fig. 6. The solid line indicates the results obtained for the interaction of the two bubbles, while the dashed curve represents the single bubble case. For the case of a single bubble, the penetration

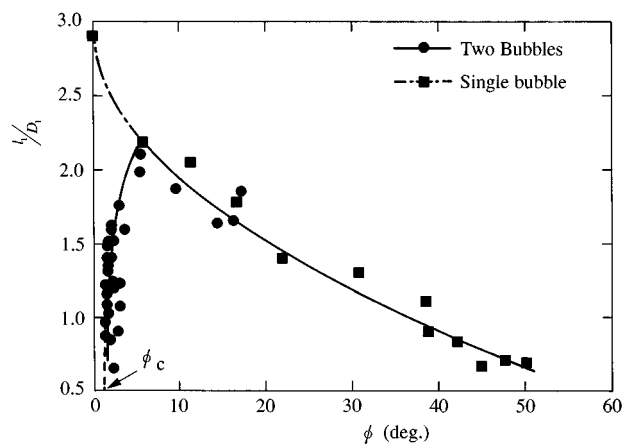


FIG. 6. Relation between the maximum jet penetration depth l_1/D_1 and incident angle ϕ : $D_1, D_2=1.88\pm0.12$ mm, $P_s=10.2\pm0.5$ MPa. The interaction of the two bubbles result is depicted with the solid curve while the dashed curve represents the single bubble result.

depth decreases with increasing ϕ , because a liquid jet is always formed in the direction of the propagation of the incident shock wave. The maximum penetration is 2.9 times as deep as the initial bubble diameter and it is achieved at $\phi=0^\circ$. In the two bubbles case the penetration depth first increases with increasing ϕ ; from ϕ_c and up to $\phi=6^\circ$, where it reaches a maximum value of $l_1/D_1=2.2$. After this peak, the value of l_1 shows a similar tendency as observed in the case of a single bubble. The increase in the penetration depth means an increase in the intensity of the bubble collapse. Therefore, the results shown in Figs. 5 and 6 indicate that when two collapsing bubbles have the same diameter, the collapse intensity can be either enhanced or relaxed by varying the initial distance separating the two bubbles.

The structure of explosives which are like emulsion is similar to the structure of granular explosives with pores.¹⁹ The pore spaces can be treated as glass microballoons having diameters of $10\text{--}100\ \mu\text{m}$. The space between the pores collapses under the impulsive pressure, which results in the cre-

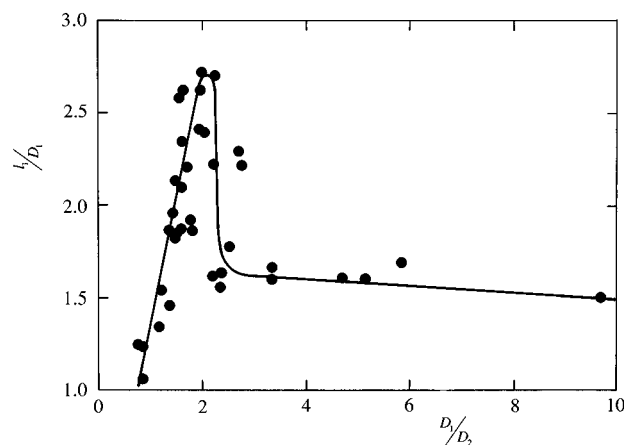


FIG. 7. Relation between the penetration depth l_1/D_1 and the ratio of D_1/D_2 ; $D_1=1.88\pm0.12$, $2S=3.95\pm0.25$ mm, $P_s=10.2\pm0.5$ MPa. l_1/D_1 increases with increasing D_1/D_2 . The bubble D_1 collapses most violently by the interaction of D_2 at $D_1/D_2\approx 2$.

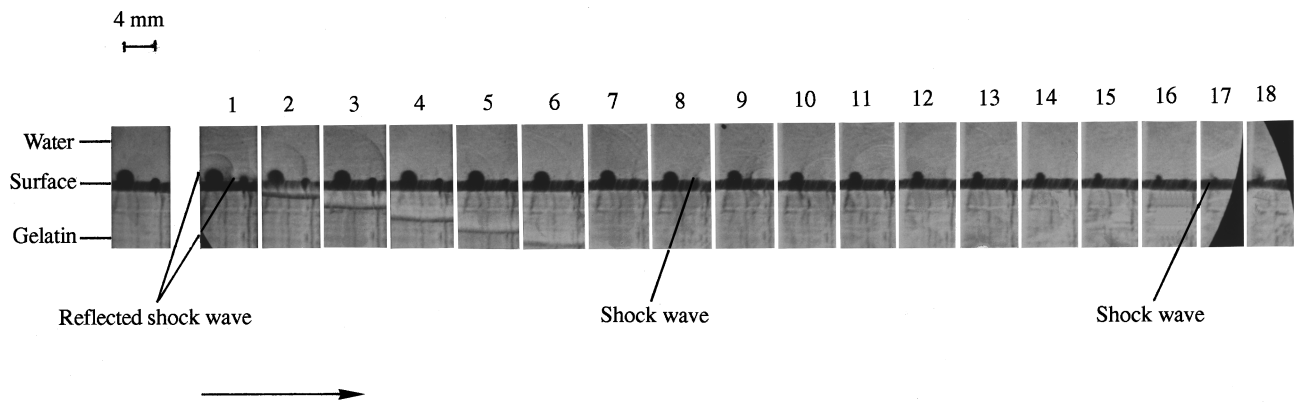


FIG. 8. Simultaneous records of the collapse of the two bubbles: $D_1/D_2=2.04$, $D_1=1.98$ mm, $D_2=0.97$ mm, $2S=3.92$ mm, $P_s=10.2\pm0.5$ MPa. Interframe time $1\ \mu\text{s}$ and exposure time $0.2\ \mu\text{s}$.

ation of a hot spot with a high pressure and a high temperature. The continuous creation of hot spots is closely related to the ignition efficiency. The above results show that the ignition efficiency will be reduced when microballoons of an identical diameter are adjacent to each other.

B. Interaction between two bubbles having different diameters

The intensity of bubble collapse is investigated by changing the ratio between D_1 and D_2 . Figure 7 shows changes in the penetration depth of the left bubble, when D_1 was kept constant at 1.88 ± 0.12 mm, $2S$ was 3.95 ± 0.25 mm, and $\phi=2.3$. The relative penetration depth l_1/D_1 increases as D_1/D_2 increases, attaining a maximum value of 2.71 at $D_1/D_2\approx 2$. After the peak, the penetration depth approaches a constant value $l_1/D_1=1.4$. In Fig. 6 the single bubble case shows $l_1/D_1=2.55$ at $\phi=2.3$. Therefore, the collapse intensity in the two bubbles case was enhanced by a factor of 1.06, compared with that of the single bubble case.

Figure 8 shows shock wave propagation recorded by the Schlieren method for $D_1/D_2=2.04$, $D_1=1.98$ mm, $D_2=0.97$ mm, and $2S=3.92$ mm. The primary shock wave loads the two bubbles and two reflected shock waves, from each bubble, are visible in the first frame of Fig. 8. A very weak reflected shock wave from the gelatin surface is noticed in this frame simply because most of the incident shock wave intensity, as previously mentioned, is transmitted into the gelatin. The propagation speed in gelatin is a little faster than that of water. Several weak shock waves are visible in the

frames and are due to the collapse of a few smaller bubbles attached to the gelatin surface. These shock waves do not affect at all dynamics of the two bubbles obtained by the present experiment, because the intensities of these shock waves are very weak. The smaller bubble D_2 collapses faster than the larger bubble D_1 , and emits a shock wave at its rebound, as can be seen in the eighth frame of Fig. 8. The shock wave which propagates spherically, attenuating approximately in proportion to $1/r$ through the liquid, loads the larger bubble as could be seen in the tenth frame of Fig. 8, where r is the propagation distance. The larger bubble collapses within $17\ \mu\text{s}$ (in the seventeenth frame of Fig. 8).

Figure 9 shows records of bubble collapse at $D_1/D_2=1.98$, where $D_1=1.91$ mm, $D_2=0.97$ mm, $2S=3.68$ mm, and the interframe time is $40\ \mu\text{s}$. In the first frame of Fig. 9 the shock wave has already impinged on the bubbles, vertically from below. The right bubble collapses completely and the left one is reaching its minimum size. In the second frame of Fig. 9, the liquid jet of the left bubble penetrates vertically into the gelatin and the right bubble starts to expand. A shock wave is emitted at the rebound phase of the right bubble between frame 1 and 2, and then it hits the left bubble.

Figure 10 shows the relationships between d_1/D_1 and D_1/D_2 , where d_1 is the contracting diameter of the larger bubble when it is loaded by the shock wave emitted from the smaller bubble. The shock wave interaction occurs at $d_1/D_1\approx 0.8$ and $D_1/D_2\approx 2$. When a bubble collapses due to shock wave interaction, the side of the bubble surface which

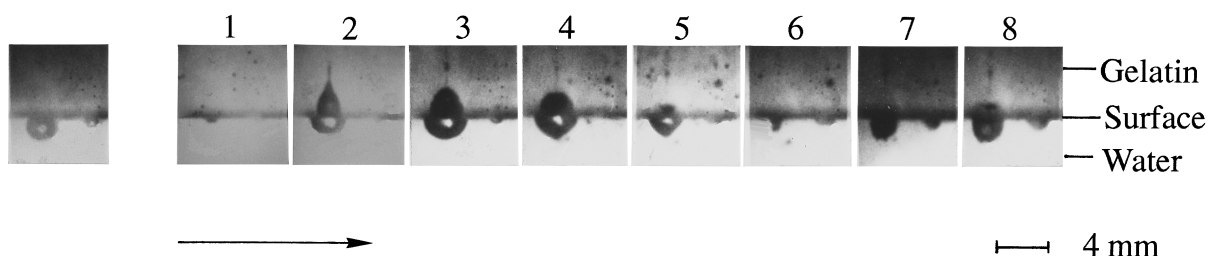


FIG. 9. Bubble collapse at the optimal condition: $D_1/D_2=1.97$, $D_1=1.91$ mm, $D_2=0.97$ mm, $2S=3.68$ mm, $P_s=10.2\pm0.5$ MPa. Interframe time $40\ \mu\text{s}$ and exposure is $8.0\ \mu\text{s}$ frame.

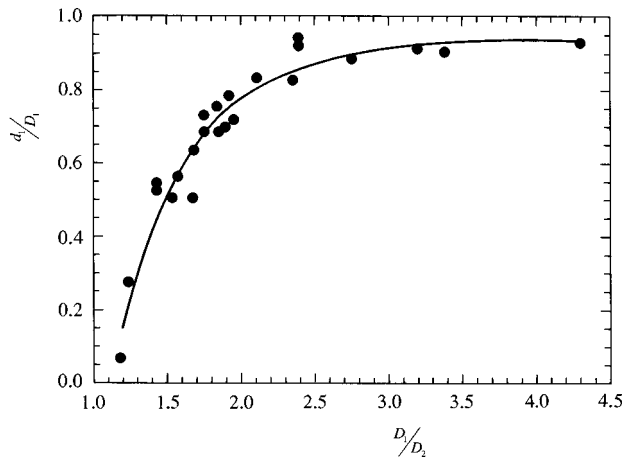


FIG. 10. Comparison between the collapsing bubble diameter d_i/D_1 and the ratio of two bubble diameters D_1/D_2 ; $D_1 = 1.99 \pm 0.12$, $2S = 3.95 \pm 0.25$ mm, $P_s = 10.2 \pm 0.5$ MPa. D_1 is loaded by the shock wave produced from the rebound of D_2 at the time when the contracting diameter of D_1 is 80% of its initial diameter.

is loaded by the shock wave is accelerated to some speed by the momentum transfer of the reflected wave. The bubble surface which is accelerated by the reflection collapses faster than the other part of the surface and a high-pressure region is generated near the accelerated surface. This results in a liquid jet penetrating in the direction of the shock wave propagation. This pressure increases due to the convergence and the nonlinear effects of the bubble collapse⁴ and attains its maximum value when the bubble approaches its minimum volume. Takayama *et al.*²⁰ visualized by double exposure holographic interferometry, drastic fringe concentration where the shock wave first impinged the bubble, showing the high-pressure generation process. The results presented above show that the bubble collapse might be enhanced at the time when the shock wave emitted from the other bubble crosses the high-pressure region produced not at the last stage but at the early stage.

In general, the bubble collapse process and the intensity of the rebound shock wave in the liquid depend on many parameters, such as the pressure history of the shock waves which hit it, the separation distance between the bubbles, the bubble diameters and shapes, the gas pressure and its properties inside the bubble (i.e., condensable or noncondensable gas), the thermal boundary layers developing both inside and outside the bubble, and the physical properties of the liquid. Further research is needed to clarify the details of the mechanism responsible for the pressure increase that accompanies the bubble-shock wave interaction.

IV. CONCLUSIONS

The interaction of two bubbles, attached to a gelatin surface, with an underwater shock wave was investigated by varying the separation distance between the two bubbles and the bubbles' diameter in order to clarify the mutual interaction between the bubbles. The following conclusions were found;

- (1) When the bubbles are beyond a critical separation distance, the directivity and the depth of the liquid jet is no longer affected by the presence of the other bubble.
- (2) The shock waves produced by the collapse of a bubble travel to adjacent collapse bubbles and enhance their collapse and the penetration they produce.

ACKNOWLEDGMENTS

This work was supported in part by a Grant-in-Aid for Developmental Scientific Research obtained from the Japanese Ministry of Education, Science, Sports and Culture No. 07557254. Their support is acknowledged with thanks.

- ¹I. Hansson and K. A. Mørch, *J. Appl. Phys.* **51**, 4651 (1980).
- ²N. Sanada, J. Ikeuchi, K. Takayama, and O. Onodera, in *Proceedings of the 14th International Symposium on Shock Tubes and Shock Waves*, edited by R. D. Archer and B. E. Milton, New South Wales, Australia, 1983, p. 405.
- ³Y. Tomita, A. Shima, and T. Ohno, *J. Appl. Phys.* **56**, 125 (1984).
- ⁴S. Fujikawa and H. Takahira, *Acustica* **61**, 188 (1986).
- ⁵Y. Tomita and A. Shima, *J. Fluid Mech.* **169**, 535 (1986).
- ⁶J. P. Dear and J. E. Field, *J. Fluid Mech.* **190**, 409 (1988).
- ⁷P. Testud-Giovannesch, A. P. Alloncle, and D. Dufresne, *J. Appl. Phys.* **67**, 3560 (1990).
- ⁸T. Kodama, Y. Tomita, K. Sato, and A. Shima, in *Proceedings of the 18th International Symposium on Shock Tubes and Shock Waves*, edited by T. Takayama, Sendai, Japan, 1991, p. 559.
- ⁹G. D. Coley and J. E. Field, *Proc. R. Soc. London* **335**, 67 (1973).
- ¹⁰J. N. Johnson, *Proc. R. Soc. London, Ser. A* **413**, 329 (1987).
- ¹¹K. Takayama, *Jpn. J. Appl. Phys.* **32**, 2192 (1993).
- ¹²A. J. Coleman, T. Kodama, M. J. Choi, T. Adams, and J. E. Saunders, *Ultrasound Med. Biol.* **21**, 405 (1995).
- ¹³Y. Tomita, T. Kodama, and A. Shima, *Appl. Phys. Lett.* **59**, 274 (1991).
- ¹⁴T. Kodama, Y. Tomita, and A. Shima, *Trans. Jpn. Soc. Mech. Eng.* **59**, 1431 (1993).
- ¹⁵K. Takayama, H. Esashi, and N. Sanada, in *Proceedings of the 14th International Symposium on Shock Tubes and Shock Waves*, edited by R. D. Archer and B. E. Milton, New South Wales, Australia, 1983, p. 553.
- ¹⁶W. F. Ballhaus, Jr. and M. Holt, *Phys. Fluids* **17**, 1068 (1974).
- ¹⁷R. H. Cole, *Underwater Explosion* (Princeton University Press, Princeton, 1948), p. 312.
- ¹⁸G. Birkhoff and E. H. Zarantonello, *Jets, Wakes and Cavities* (Academic, New York, 1957).
- ¹⁹N. K. Bourne and J. E. Field, *J. Fluid Mech.* **259**, 149 (1994).
- ²⁰K. Takayama, A. Abe, and K. Tanaka, in *Proceedings of the IUTAM Symposium*, edited by G. E. A. Meier and P. A. Thompson (Göttingen, Germany, 1989), p. 91.